Mon. Not. R. Astron. Soc. **000**, 1–11 (2004) Printed 2 February 2008 (MN LATEX style file v2.2)

Relativistic spectral features from X-ray illuminated spots and the measure of the black hole mass in AGN

M. Dovčiak,[1,2] S. Bianchi,[3] M. Guainazzi,[4] V. Karas[1,2] and G. Matt[3]

[1] *Astronomical Institute, Academy of Sciences of the Czech Republic, Boční II, CZ-140 31 Prague, Czech Republic*
[2] *Charles University, Faculty of Mathematics and Physics, V Holešovičkách 2, CZ-180 00 Prague, Czech Republic*
[3] *Dipartimento di Fisica, Università degli Studi "Roma Tre", Via della Vasca Navale 84, I-00146 Roma, Italy*
[4] *XMM Science Operation Center, RSSD-ESA, VILSPA, Apartado 50727, E-28080 Madrid, Spain*

Accepted .... Received ...

ABSTRACT

Narrow spectral features in the 5–6 keV range were recently discovered in the X-ray spectra of a few active galactic nuclei. We discuss the possibility that these features are due to localized spots which occur on the surface of an accretion disc following its illumination by flares. We present detailed line profiles as a function of orbital phase of the spot and its radial distance from a central black hole. Comparison of these computed profiles with observed features can help to estimate parameters of the system. In principle this method can provide a powerful tool to measure the mass of super-massive black holes in active galactic nuclei. By comparing our simulations with the *Chandra* and *XMM–Newton* results, we show, however, that spectra from present generation X-ray satellites are not of good enough quality to fully exploit the method and determine the black hole mass with sufficient accuracy. This task has to be deferred to future missions with high throughput and high energy resolution, such as *Constellation–X* and *Xeus*.

Key words: line: profiles – relativity – galaxies: active – X-rays: galaxies

1 INTRODUCTION

Relativistic iron line profiles may provide a powerful tool to measure the mass of the black hole in active galactic nuclei (AGNs) and Galactic black hole candidates. To this aim, Stella (1990) proposed to use temporal changes in the line profile following variations of the illuminating primary source (which at that time was assumed to be located on the disc axis for simplicity). Along the same line of thought, Matt & Perola (1992) proposed to employ, instead, variations of the integrated line properties such as equivalent width, centroid energy and line width. These methods are very similar conceptually to the classical reverberation mapping method, widely and successfully applied to optical broad lines in AGNs. Sufficiently long monitoring of the continuum and of the line emission is required, as well as large enough signal-to-noise ratio. However, the above-mentioned methods have not provided many results yet. Even in the best studied case of the Seyfert galaxy MCG–6-30-15, the mass estimate is hard to obtain due to the apparent lack of correlation between the line and continuum emission (Fabian et al. 2002). It was suggested that also these complications are possibly caused by an interplay of complex general relativistic effects (Miniutti et al. 2003). X-ray spectra from high throughput and high energy resolution detectors should resolve the problem of interpretation of observed spectral features. However, before such high quality data are available it is desirable to examine existing spectra and attempt to constrain physical parameters of the models.

A simple, direct and potentially robust way to measure the black hole mass would be available if the line emission originates at a given radius and azimuth, as expected if the disc illumination is provided by a localized flare just above the disc (possibly due to magnetic reconnection), rather than a central illuminator or an extended corona. If a resulting 'hot spot' co-rotates with the disc and lives for at least a significant part of an orbit, by fitting the light curve and centroid energy of the line flux, the inclination angle $\theta_{\rm o}$ and the orbit radius could be derived (radius in units of the gravitational radius $r_{\rm g}$). Further, assuming Keplerian rotation, the orbital period is linked with radius in a well-known manner. The equation for the orbital period then contains the black hole mass $M_\bullet$ explicitely, and so this parameter can be determined, as discussed later.

Hot spots in AGN accretion discs were popular for a while, following the finding of apparent periodicity in the X-ray emission of the Seyfert 1 galaxy NGC 6814. They, however, were largely abandoned when this periodicity was demonstrated to be associated with an AM Herculis system

in the field of view rather than the AGN itself (Madejski et al. 1993). Periodicities in AGNs were subsequently reported in a few sources (Iwasawa et al. 1998; Lee et al. 2000; Boller et al. 2001). The fact that they were not confirmed in different observations of the same sources is not surprising – quite on the contrary, it would be hard to imagine a hot spot surviving for several years.

Recently, the discovery of narrow emission features in the X-ray spectra of several AGNs (Turner et al. 2002, 2004; Guainazzi 2003; Yaqoob et al. 2003) has renewed interest in hot spots. There is a tentative explanation (even if not the only one) for these features, typically observed in the 5–6 keV energy range, in terms of iron emission produced in a small range of radii and distorted by joint action of Doppler and gravitational shift of photon energy. Iron lines would be produced by localized flares which illuminate the underlying disc surface, producing the line by fluorescence. Indeed, the formation of magnetic flares on the disc surface is one of the most promising scenarios for the X-ray emission of AGNs. A particularly strong flare, or one with a very large anisotropic emission towards the disc, could give rise to the observed features. Small width of the observed spectral features implies that the emitting region must be small, and that it is seen for only a fraction of the entire orbit (either because the flare dies out, or because emission goes below detectability, see next section). If the flares co-rotate with the disc and if they last for a significant part of the orbit, it may be possible by observing their flux and energy variations with phase to determine the orbital parameters, and thence $M_\bullet$.

In section 2 we illustrate the basic properties of the line emitted from an orbiting, illuminated spot. In section 3 we compare calculations with the relevant narrow-line features reported in several AGNs. Section 4 is devoted to the summary and perspectives.

2 LINE PROFILES FROM AN ORBITING, X-RAY ILLUMINATED SPOT

The basic properties of line emission from the innermost regions of an accretion disc around a black hole are well-known (see e.g. Reynolds & Nowak 2003; Fabian et al. 2000 for recent reviews). Let us here briefly summarize several formulae most relevant to our purposes.

If r is the orbital radius and a is the dimension-less black hole angular momentum, the orbital period of matter co-rotating along a circular trajectory $r = \text{const}$ around the black hole is given by (Bardeen, Press & Teukolsky 1972)

$$T_{\rm orb} \doteq 310 \left(r^{\frac{3}{2}} + a\right) \frac{M_\bullet}{10^7 M_\odot} \quad [\text{sec}], \tag{1}$$

as measured by a distant observer. We express lengths in units of the gravitational radius $r_{\rm g} \equiv GM_\bullet/c^2 \doteq 1.48 \times 10^{12} M_7$ cm, where M_7 is the mass of the black hole in units of 10^7 solar masses. Angular momentum a (per unit mass) is in geometrized units ($0 \le a \le 1$). See e.g. Misner, Thorne & Wheeler (1973) for useful conversion formulae between geometrized and physical units.

The innermost stable orbit, $r_{\rm ms}$, occurs for an equatorial disc at radius

$$r_{\rm ms} = 3 + Z_2 - \left[(3 - Z_1)(3 + Z_1 + 2Z_2) \right]^{\frac{1}{2}}, \tag{2}$$

where $Z_1 = 1 + (1 - a^2)^{\frac{1}{3}}[(1 + a)^{\frac{1}{3}} + (1 - a)^{\frac{1}{3}}]$ and $Z_2 = (3a^2 + Z_1^2)^{\frac{1}{2}}$; $r_{\rm ms}$ spans the range of radii from $r = 1$ ($a = 1$, i.e. the case of a maximally rotating black hole) to 6 ($a = 0$, a static black hole). Rotation of a black hole is believed to be limited by an equilibrium value $a \doteq 0.998$ because of the capture of photons from the disc (Thorne 1974). This would imply $r_{\rm ms} \doteq 1.23$. Different models of accretion can result in somewhat different limiting values of a and the corresponding $r_{\rm ms}(a)$. Notice that in the static case, the radial dependence $T_{\rm orb}(r)_{|a=0}$ is identical to that in purely Newtonian gravity.

In order to compute a synthetic profile of an observed spectral line one has to link the points of emission in the disc with corresponding pixels in the detector plane at spatial infinity. This can be achieved by solving the ray-tracing problem in curved space-time of the black hole. Appropriate methods were discussed by several authors; see Reynolds & Nowak (2003) for a recent review and for further references. This way one finds the redshift factor, which determines the energy shift of photons, the lensing effect (i.e. the change of solid angle due to strong gravity), and the effect of aberration (which influences the emission direction of photons from the disc; this must be taken into account if the intrinsic emissivity is non-isotropic). We consider these effects in our computations, assuming a rotating (Kerr) black hole spacetime (Misner et al. 1973). We also consider time of arrival of photons originating at different regions of the disc plane. Variable travel time results in mutual time delay between different photons, which can be ignored when analyzing time-averaged data but it may be important for time-resolved data.

Assuming purely azimuthal Keplerian motion of a spot, one obtains for its orbital velocity (with respect to a locally non-rotating observer at corresponding radius r):

$$v^{(\phi)} = \frac{r^2 - 2a\sqrt{r} + a^2}{\sqrt{\Delta}\,(r^{3/2} + a)}. \tag{3}$$

In order to derive time and frequency as measured by a distant observer, one needs to take into account the Lorentz factor associated with this orbital motion,

$$\Gamma = \frac{\left(r^{3/2} + a\right)\sqrt{\Delta}}{r^{1/4}\,\sqrt{r^{3/2} - 3r^{1/2} + 2a}\,\sqrt{r^3 + a^2 r + 2a^2}}. \tag{4}$$

Corresponding angular velocity of orbital motion is $\Omega = (r^{3/2} + a)^{-1}$, which also determines the orbital period in eq. (1). The redshift factor g and the emission angle ϑ (with respect to the normal direction to the disc) are then given by

$$g = \frac{\mathcal{C}}{\mathcal{B} - r^{-3/2}\xi}, \quad \vartheta = \arccos\frac{g\sqrt{\eta}}{r}, \tag{5}$$

where $\mathcal{B} = 1 + ar^{-3/2}$, $\mathcal{C} = 1 - 3r^{-1} + 2ar^{-3/2}$; ξ and η are constants of motion connected with the photon ray in an axially symmetric and stationary spacetime.

For practical purposes formula (1) with $a = 0$ is accurate enough also in the case of a spinning black hole, provided that r is not very small. For instance, even for $r = 6$ (the last stable orbit in Schwarzschild metric), $T_{\rm orb}(r_{\rm ms})$ calculated for a static and for a maximally rotating ($a = 1$) black hole differ by about 6.8%. The relative difference decreases, roughly linearly, down to 1.1% at $r = 20$. This implies that eq. (1) can be used in most cases to estimate the

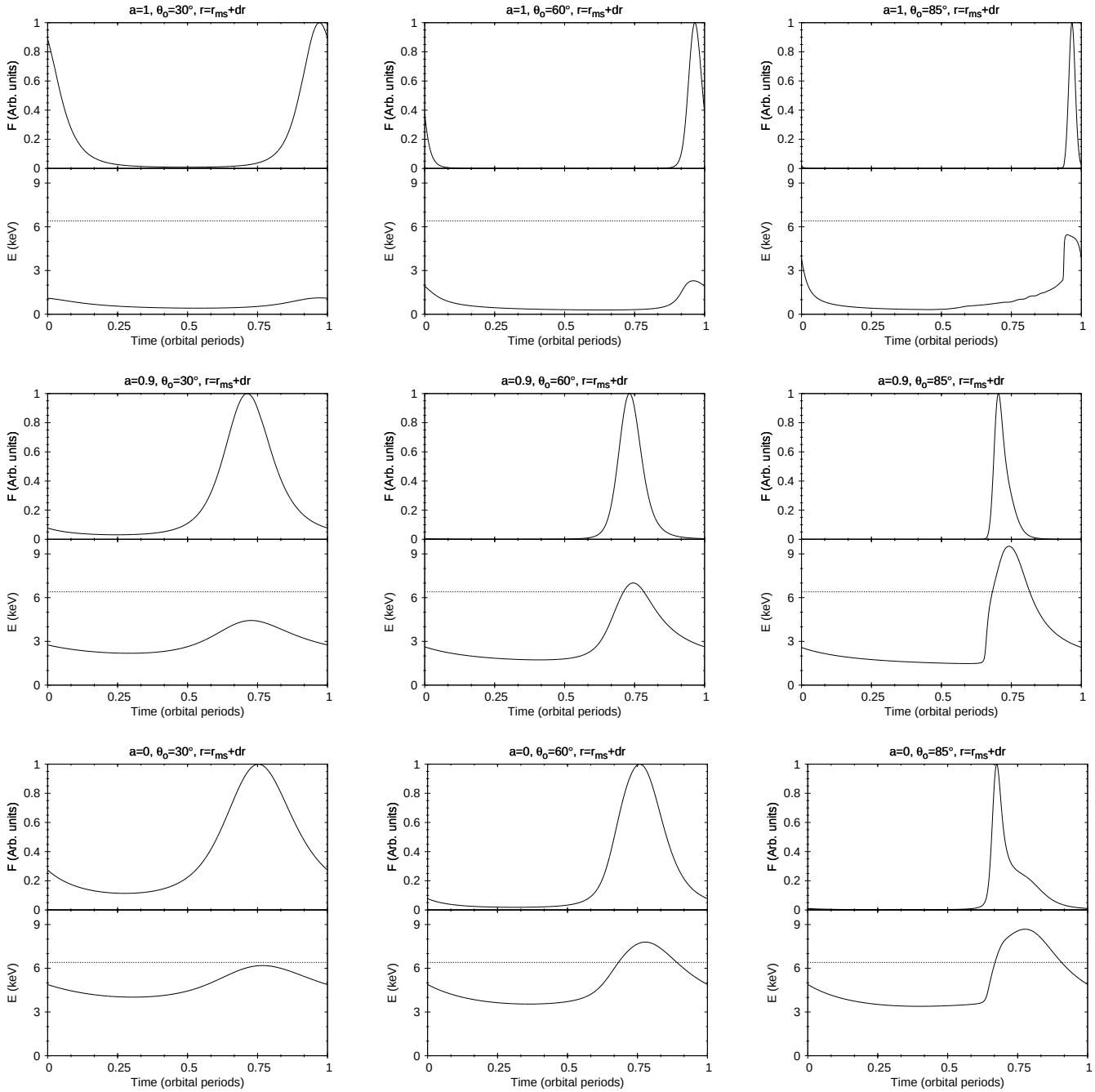

Figure 1. Line flux and centroid energy as functions of the orbital phase of a spot, for three values of angular momentum ($a = 1$, 0.9, and 0) and three inclination angles ($\theta_{\rm o} = 30^\circ$, 60°, 85°). The center of the spot is located at radial distance r, which corresponds to the last stable orbit $r_{\rm ms}(a)$ for that angular momentum plus a small displacement given by the spot radius, dr. The intrinsic energy of the line emission is assumed to be at 6.4 keV (indicated by a dotted line). Prograde rotation is assumed. Time is expressed in orbital periods.

black hole mass even if the angular momentum is not known (deviations are relevant only for $r < 6$, when the radius itself can be used to constrain the allowed range of a).

Various pseudo-Newtonian formulae have been devised for accreting black holes to model their observational properties, which are connected with the orbital motion of surrounding matter (e.g. Abramowicz et al. 1996; Artemova, Björnsson & Novikov 1996; Semerák & Karas 1999). Although this approach is often used and found to be practical, we do not employ it here because error estimates are not possible within the pseudo-Newtonian scheme.

Due to Doppler and gravitational energy shift the line shape changes along the orbit. Centroid energy is redshifted with respect to the rest energy of the line emission for most of the orbit. Furthermore, light aberration and bending cause the flux to be strongly phase–dependent. These effects are shown in Figures 1–2. In these plots, the arrival time of photons is defined in orbital periods, i.e. scaled with $T_{\rm orb}(r; a)$. The orbital phase of the spot is of course linked

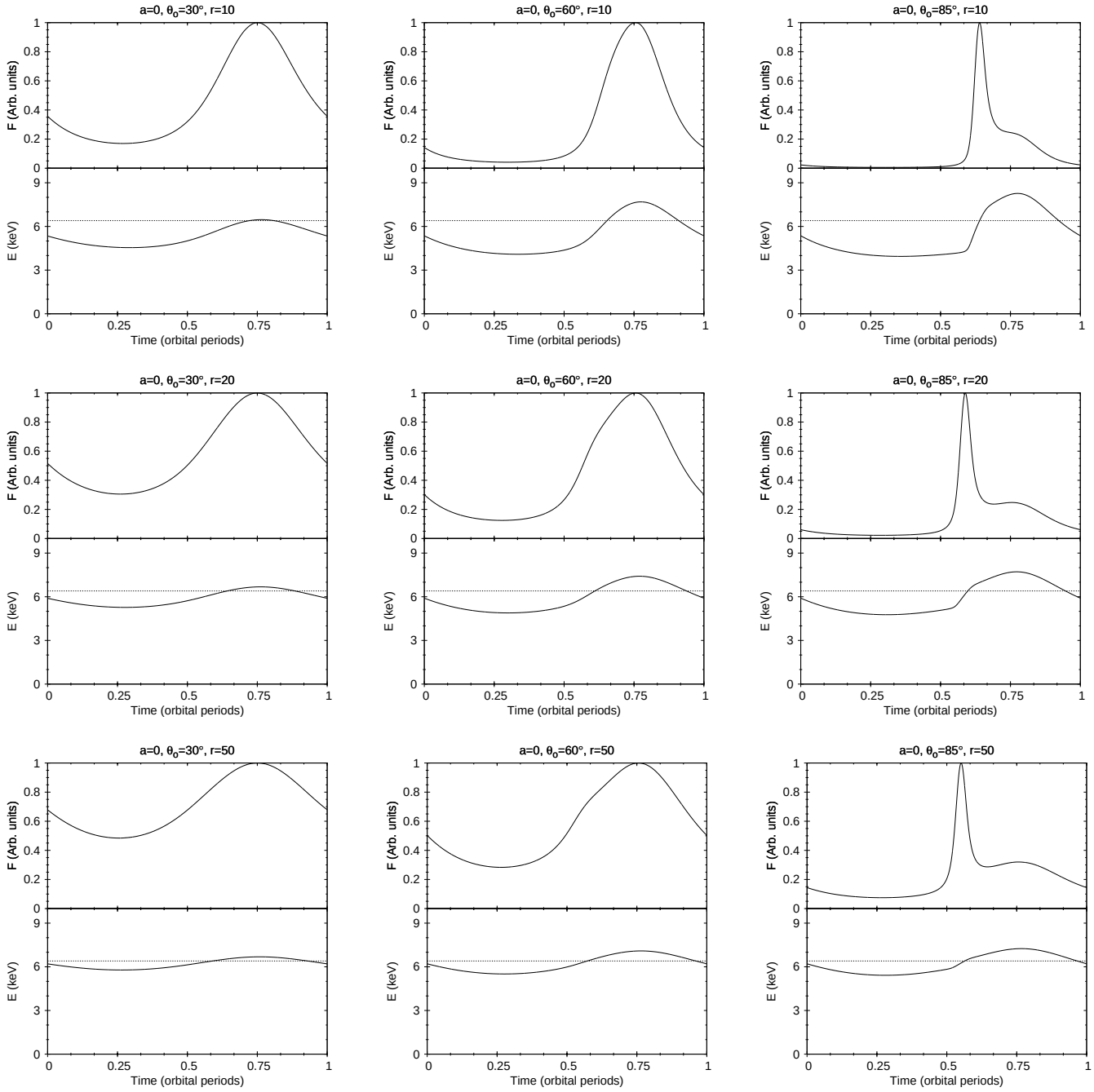

Figure 2. The same as the previous figure, but with $a = 0$ and $r = 10$ (top), 20 (middle), and 50 (bottom).

with the azimuthal angle in the disc, but the relation is made complex by time delays which cannot be neglected, given the large velocities of the orbiting matter and frame-dragging effects near the black hole. Here, zero time corresponds to the moment when the center of the spot was at the nearest point on its orbit with respect to the observer (a lower conjunction). The plots in Fig. 1 refer to the case of a spot circulating at the innermost stable orbit $r_{\rm ms}(a)$ for $a = 0$, 0.9 and 1. The effect of black hole rotation becomes prominent for almost extreme values of a; one can check, for example, that the difference between cases $a = 0$ and $a = 0.5$ is very small.

Worth remarking is a large difference in the orbital phase of maximum emission between the extreme case, $a \to 1$, in contrast to the non-rotating case, $a \to 0$. The reason is that for large a the time delay and the effect of frame-dragging on photons emitted behind the black hole are very substantial. It is also interesting to note that, for very high inclination angles, most of the flux comes from the far side of the disc, due to very strong light bending, as pointed out by Matt et al. (1992, 1993) and examined further by many authors who performed detailed ray tracing, necessary to determine the expected variations of the line flux and shape. A relatively simple fitting formula has been

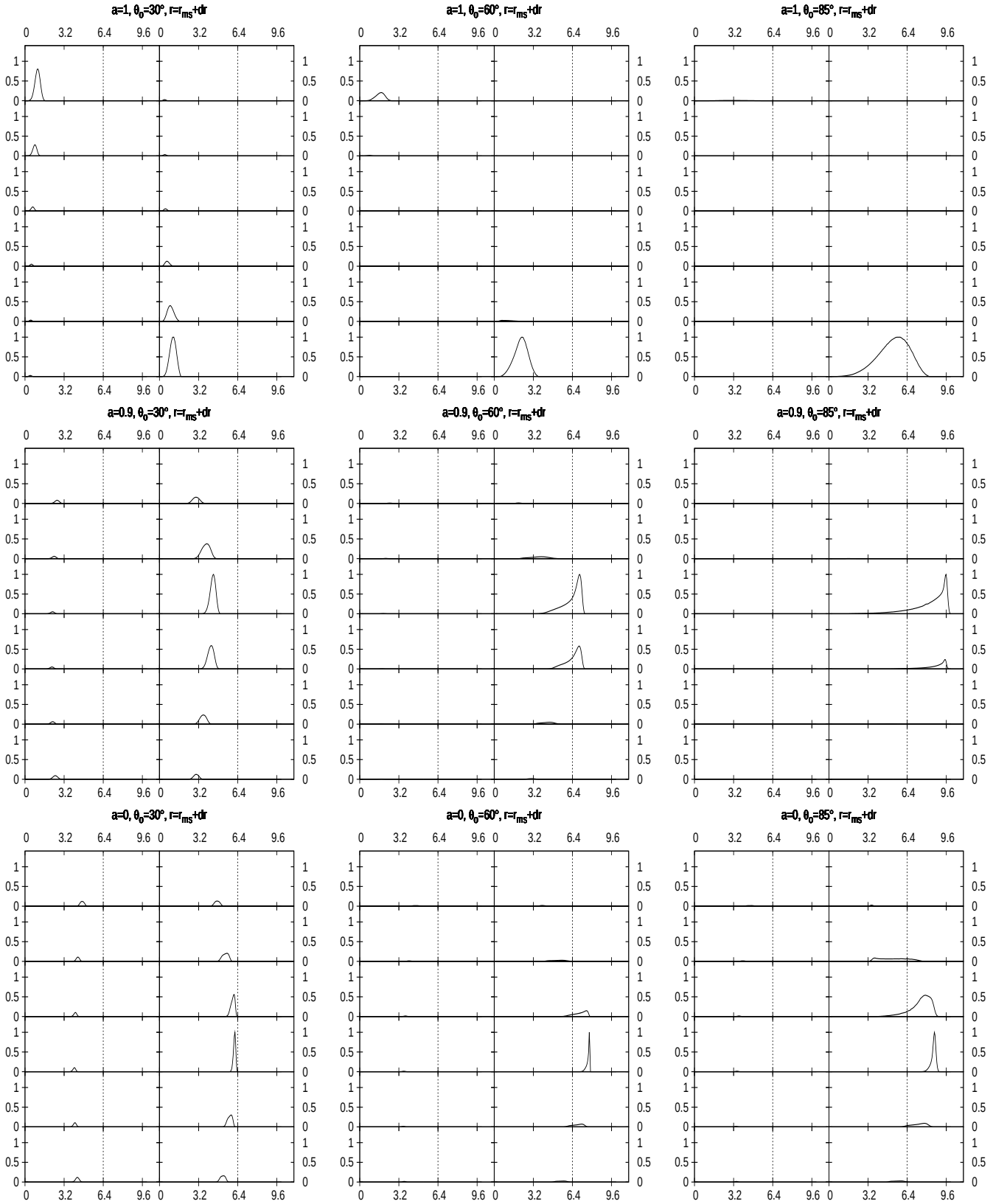

Figure 3. Line profiles integrated over twelve consecutive temporal intervals of equal duration. Each interval covers 1/12 of the orbital period at corresponding radius. As explained in the text, top-left frame of each panel corresponds to the spot being observed at the moment of passing through lower conjunction. Energy is on abscissa (in keV). Observed photon flux is on ordinate (arbitrary units, scaled to the maximum flux which is reached during the complete revolution of the spot). Notice the occurrences of narrow and prominent peaks which appear for relatively brief fraction of the total period. Vertical dotted lines indicate the line rest frame energy.

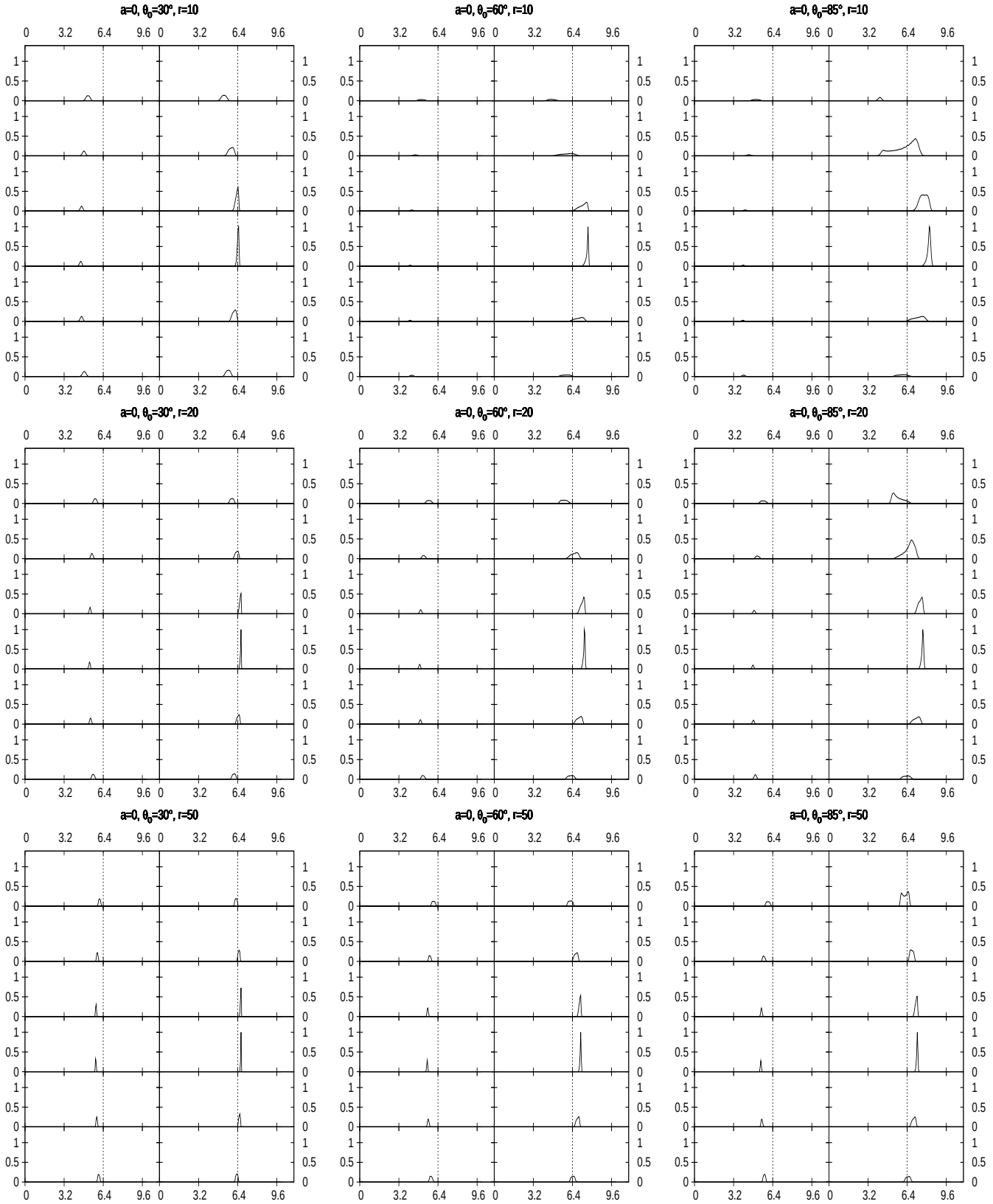

Figure 4. The same as in previous figure, but with $r = 10$ (top), 20 (middle), and 50 (bottom). The black hole was assumed non-rotating, $a = 0$ in this figure.

also derived (Karas 1996) and can be useful for practical computations.

Three more orbits (centered at $r = 10$, 20 and 50) are shown for $a = 0$ (Figure 2). As said above, at these radii differences between spinning and static black holes are small. Indeed, it can be verified that the dependence on a is only marginal if $r \gtrsim 20$, and so it can be largely neglected for present-day measurements.

In Figures 3–4 we show the actual form of the line profiles for the same sets of parameters as those explored in Figs. 1–2. The entire revolution was split into twelve different phase intervals. The intrinsic flux I is assumed to decrease exponentially with the distance dr from the centre of the spot (i.e. $\log I \propto -[\kappa\,\mathrm{d}r/r]^2$, where r is the location of the spot centre and $\kappa \sim 10$ is a constant). The illumination is supposed to cease at distance dr away from the spot centre, which also defines the illuminated area in the disc. Let us remark that we concentrate on a spectral line which is intrinsically narrow and unresolved in the rest frame of the emitting medium. Such a line can be produced by a spot which originates due to sharply localized illumination by flares, as proposed and discussed by various authors (e.g. Haardt, Maraschi & Ghisellini 1994; Poutanen & Fabian 1999; Merloni & Fabian 2001).

Very recently, Czerny et al. (2004) have examined the induced rms variability in the flare/spot model with relativistic effects. In this scheme, the actual size of the spot is linked with the X-ray flux, which is produced in the flare, and with the vertical height at which the flare occurs above the disc plane. These quantities are obviously model-dependent. Czerny et al. (2004) computations provided different cases with the spot size ranging from a fraction of $r_{\rm g}$ to several units of $r_{\rm g}$. Our computations can also simulate the observed features with the spot size as a free parameter, but with present data we cannot constrain this parameter with sufficient accuracy. Obviously, the idea of narrow spectral features favours small size of the spot, as large spots would produce broader features and they would be more prone to rapid destruction. Hence, we fix the spot size somewhat arbitrarily at a lower boundary, $\mathrm{d}r = 0.2r$.

In many cases, and especially for small radii and intermediate to large inclination angles, the line emission comes from a relatively minor fraction of the orbit. This implies in practice that for observations with a *moderate signal-to-noise ratios, only a narrow blue horn can be visible, and only for a small part of the orbit.* These large and rapid changes of the line shape get averaged when integrating over the entire orbit, and so an important piece of information is missing in the mean spectra. The line profiles integrated over the whole revolution are shown in Figure 5. Effectively, the mean profile of a spot is identical to the profile of an annulus whose radius is equal to the distance of the spot centre and the width is equal to the spot size.

3 OBSERVATIONAL EVIDENCE FOR NARROW, RELATIVISTIC FEATURES

Recently, interesting narrow emission features have been discovered in several AGNs. They occur in X-ray spectra, mostly (but not exclusively) at energies lower than 6.4 keV, which is the intrinsic energy of the neutral iron Kα fluorescent line in a frame co-moving with the emitting medium. The sources are: NGC 3516 (Turner et al. 2002), ESO 198-G024 (Guainazzi 2003), NGC 7314 (Yaqoob et al. 2003), and Mrk 766 (Turner et al. 2004). Possible interpretations include lines from spallation products of iron (Skibo 1997), and shifted iron lines. In the spallation model, the strongest expected line (after the iron line) is the Cr Kα line at 5.4 keV, the second strongest being the Mn Kα line at 5.9 keV (Skibo 1997). Some of the observed features do not match these energies (see below), and hence an energy shift is required. However, a 6.4 keV line is always present, suggesting that the *primary line is not shifted*. We therefore consider in most cases the spallation model an unlikely explanation.

Shift of the iron line may be due either to fast moving ejecta, or to orbiting material. Quality of the present data is not good enough to discriminate between these two options. In the case of the orbiting spot model presented in this paper, narrow features should occur in spectra because the two horns are often sharp. The blue horn is expected to be brighter than the red one (see Fig. 5). For insufficient signal-to-noise observations, only the blue horn may be actually visible, the remaining of the profile getting easily confused with continuum. It is worth noting, however, that this argument does not apply to the extreme case of $a \to 1$, $r \to r_{\rm ms}$, where the profile is very broad and with no sharp peak at all. Therefore, the observed features cannot arise from a spot orbiting in the last stable orbit of a maximally rotating black hole.

In the following we will recapitulate the observational evidence for these features, and derive the system parameters in the framework of the orbiting spot scenario. For all these sources past claims of the presence of 'classical' relativistic lines do exist, although only for NGC 3516 the evidence seems to be robust. The equivalent widths (EW) of the narrow features are typically of a few tens of eV. Even allowing for the fact that only the blue horn is probably observed, this implies that the spot itself contributes just a moderate fraction of the total X-ray luminosity. In our estimate we assumed an isotropically illuminating flare (for definiteness of the model). It is worth noting that non-isotropic illumination in the local frame co-moving with the flare is also possible, and it would influence the predicted profiles especially if they originate at small distance from the black hole. A relatively steady contribution to the signal is therefore required. Detailed temporal analysis of spectral features simultaneously with the continuum fluxes would be necessary in order to accurately test the scheme. Such analysis should also provide further constraints on the angular distribution of illuminating spots. This is, however, beyond the capabilities of present instruments, and therefore in the following we limit ourselves only to the discussion of spectral features.

The comparison between the model and the observation will be made assuming that the emitted line has the rest-energy of 6.4 keV, as measured in the local reference frame attached to the emitting matter. It means that iron is not ionized more than Fe XVI, a plausible assumption under usual conditions in accretion discs in AGNs. However, significant ionization of iron cannot be ruled out completely, especially below a flare, in which case the rest-energy of the line could be larger (up to 6.97 keV for H–like iron). If this is the case, the energy shift must be also larger in order to achieve

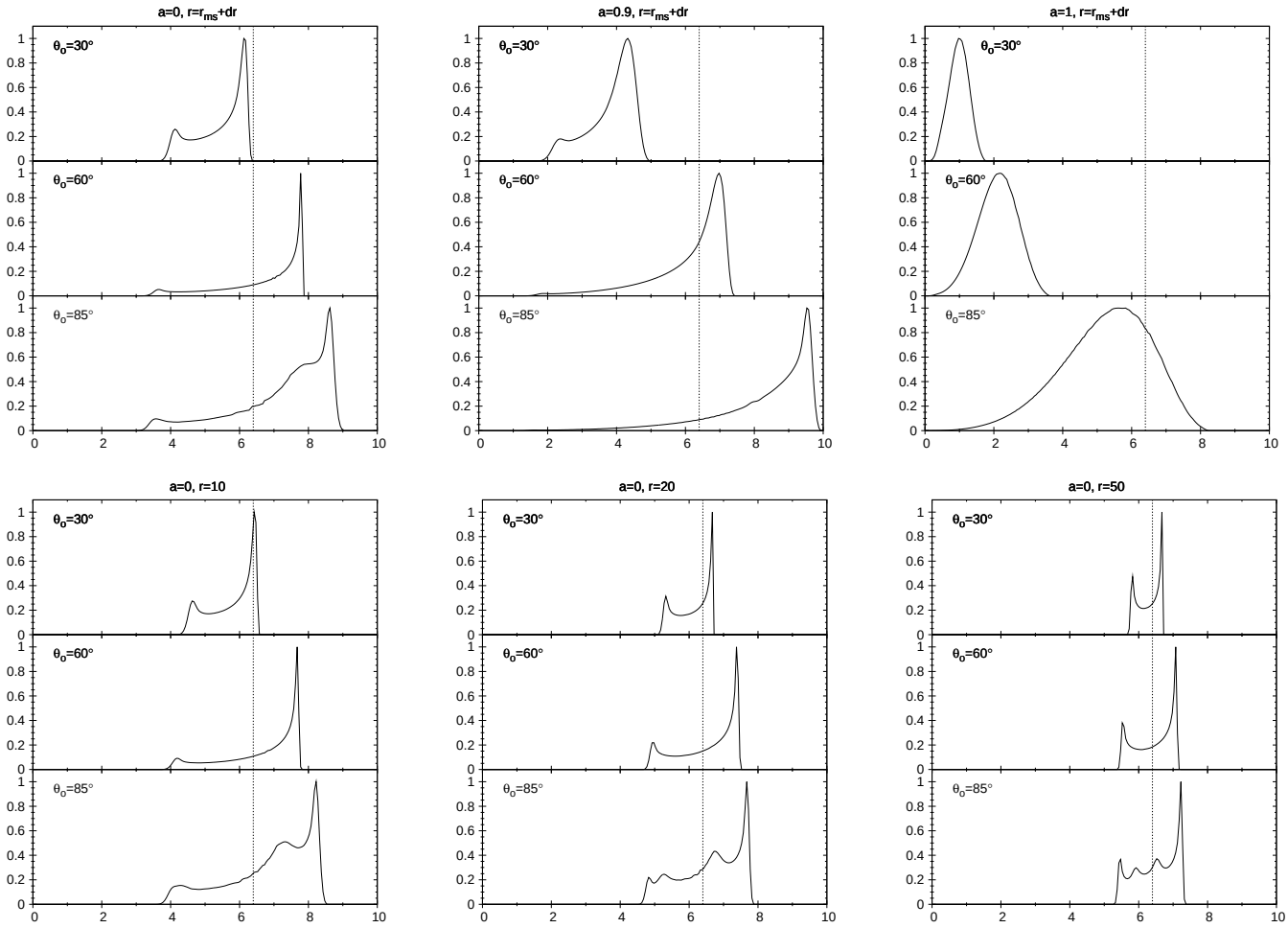

Figure 5. Time–averaged synthetic spectra in terms of photon flux (in arbitrary units) versus energy (in keV). These profiles represent the mean, background-subtracted spectra of the Fe Kα iron-line originating from spots at different radii. Top panels correspond to $r = r_{\rm ms}$ and $a = 0$ (left), $a = 0.9$ (middle), and $a = 1$ (right). In bottom panels we fix $a = 0$ and choose $r = 10$, 20, and 50, respectively (other values of a give very similar profiles). Three consecutively increasing values of observer inclination $\theta_{\rm o}$ are shown, as indicated inside the frames.

the same observed energy of the spectral feature, and this implies either a smaller radius or a smaller inclination angle with respect to the neutral line. Therefore, the values we will obtain for these two parameters should be considered as upper limits. This conclusion is rather straightforward but worth emphasizing: if the source inclination is estimated independently, then the adopted method can provide the *upper value to the radius where the line emission originates*. Once the spectral resolution and sensitivity of the available instruments are improved, subtle differences will be exploited and the ionization state will be determined more precisely. For instance, the neutral fluorescent line and the H–like resonant lines are actually doublets, with different energy separation, which is not true for the resonant He–like line, not mentioning the shape for the Compton Shoulder and the ratio between the Kβ and Kα lines, which are dependent on ionization. There is thus some prospect to distinguish these cases in future.

It is worth noting that the expected narrow-line variability should be associated with fluctuations of the X-ray continuum, because both spectral components have common origin in this model. Indeed, power spectral analysis of accreting black-hole sources shows clear evidence for such variability on vastly different time-scales (e.g. Markowitz et al. 2003 and references therein). Recently, Collin et al. (2003) examined theoretical spectra of the flare model, which is basically a generalization of the lamp-post scheme to the case of a large number of independent primary sources occurring off-axis, just above the disc plane. It will be interesting to explore in detail relations between continuum variability and the properties of spectral features. This is however beyond the scope of this paper, and it is deferred to a future work. We just note here that for two sources from our sample, no variations of the feature during the observations are apparent, which implies that neither variations in the continuum are expected. For the other two sources there is indeed evidence for variations in the feature flux, and so for them the relation with continuum variations will be briefly discussed in relevant sections below.

3.1 NGC 3516

NGC 3516 is one of the best studied Seyfert 1 galaxies, and one of the best cases of 'classical', broad iron line from a

relativistic disc (ASCA: Nandra et al. 1999; *XMM–Newton*: Turner et al. 2002). Evidence for a (possibly gravitationally) redshifted iron absorption line in the ASCA spectrum was also reported by Nandra et al. (1999).

NGC 3516 was observed twice by *XMM–Newton*, on April 2001 and November 2001; both observations were partly overlapping with *Chandra* ones. The November 2001 observations were published by Turner et al. (2002). The *Chandra*/HETG and *XMM–Newton* spectra exhibit five narrow lines. One line is at 6.4 keV (possibly originating in distant matter), two lines are seen bluewards (at 6.53 and 6.84–6.97 keV, the latter feature being variable and recorded by *XMM–Newton* only), and two lines are redwards (5.57 and 6.22 keV, the former detected by *Chandra* only) of the rest frame iron line energy. Turner et al. (2002) interpret these features as the two horns of annular emission from $r = 35$ and $r = 175$, assuming inclination angle of $\theta_{\rm o} = 38^\circ$ (Wu & Han 2001; this is actually the angle estimated for the broad-line region (BLR) clouds distribution; the statistical error the authors quote is $\pm 8^\circ$). Note, however, that the black hole mass in NGC 3516 is estimated to be $M_\bullet = 2.3 \times 10^7 M_\odot$ (based on velocity dispersion; Wu & Han 2001). This implies an orbital period of $T_{\rm orb} = 150$ ks for $r = 35$, and $T_{\rm orb} = 1650$ ks for $r = 175$. The former value of $T_{\rm orb}$ is comparable while the latter is significantly longer than the total *XMM–Newton* and *Chandra* observing time (about 180 ks). Both red and blue features have been detected in the 75 ks *Chandra* observation alone. Therefore, the annular emission must be steady, and not simply a consequence of integration over time of an orbiting spot signal. It is very hard to imagine a physical situation in which this can occur. Alternatively, the red and blue features may be independent one another, the former being the blue horns from spots near the black hole, the latter being emitted at large radii (time variation of the line centroid for one of the blue features is indeed suggestive of a spot orbiting with a period comparable or longer than the exposure time).

We analysed the April 2001 *XMM–Newton* and *Chandra* observations (see also Bianchi et al. 2004). We divided the ∼74 ks long *XMM–Newton* exposure into three about equally spaced time intervals, about 17 ks each after removing periods of high background. In all three time intervals a narrow feature is observed at energy 6.01 ± 0.04, 6.11 ± 0.08 and 6.04 ± 0.11 keV, respectively (corresponding upper limits for σ are uncertain; we obtained values of $\sigma = 0.17$, 0.25 and 0.88 keV, respectively). The equivalent widths of these lines are EW = 40, 39 and 21 eV. The centroid energy of the feature is consistent with being constant as well as the flux (even if in the third interval the detection is marginal: the confidence levels at which the feature is detected are 99.96%, 99.83% and 88.15%, respectively, according to the F-test). Indeed, summing the three time intervals together yields an energy of 6.08 ± 0.03 (the feature is significant at the 99.99% confidence level). We will call it the 'red' feature. In all time intervals a narrow iron line at 6.4 keV is also found which may originate in distant matter, while no evidence for the features detected by Turner et al. (2002) in the November 2001 observations is present. In the 73 ks *Chandra* observation, instead, there is no evidence for features other than the 6.4 keV line. The upper limit to the flux of a narrow line at 6.1 keV is, however, consistent with the flux measured in the *XMM–Newton* observation.

In our approach, the constancy in energy of the feature suggests that the orbital period of the emitting annulus is lower than the exposure time of a single interval, so that we are averaging the profile over one or more orbits. Dividing further in time the observation is not possible, as the signal-to noise ratio becomes too small. This feature could be the blue horn of a $r \sim 6$ annulus profile (the rest of the line profile being too faint to be detectable). Corresponding inclination angle is slightly larger than $\theta_{\rm o} = 30^\circ$ (cp. Fig. 5). Indeed, a fit with a relativistic disc model (DISKLINE in XSPEC), and with inner and outer radii fixed to $r = 6$ and 7, respectively, comes out as good as the fit with a simple Gaussian line. The best fit inclination angle is $\theta_{\rm o} = 31^\circ$. In this case, the orbital period is about 10 ks, and for each time interval we would be averaging over almost two orbits.

Alternatively, the 'red' feature may be the red horn of a line profile in which the 6.4 keV line is the 'blue' horn. Fitting the spectrum of the whole observation with the DISKLINE model gives inclination $\theta_{\rm o} = 24^\circ$ and inner and outer radii of $r = 12$ and 15.6, respectively. At these radii the orbital period is about $T_{\rm orb} = 30$ ks, i.e. more than the observing time for each time interval, and so an orbiting spot cannot provide the observed profile and we have to resort to the rather unpalatable steady annular emission. Moreover, the statistical quality of the fit is poorer, than with a double Gaussian (the latter fit giving an improvement at the 99.95% confidence level), and the energy of the iron line, both in *XMM–Newton* and *Chandra* (Turner et al. 2002) is suspiciously close to the rest energy value. We therefore consider more likely that the 6.4 keV line originates in distant matter not affected by relativistic effects (such as the Broad Line Region or the 'torus'), and that the red feature is therefore the blue horn of a $r \sim 6$ orbiting spot.

3.2 ESO 198-G024

The Seyfert 1 galaxy ESO 198-G024 has been observed by all major X-ray satellites. Behaviour of its 6.4 keV iron line is rather puzzling: it was found to be narrow in the ASCA spectrum and broad in the first *XMM–Newton* observation (Guainazzi 2003).

The source was in fact observed by *XMM–Newton* twice: (i) on December 1st, 2000 (Guainazzi 2003) and (ii) on January 24th, 2001 (Porquet et al. 2003; Bianchi et al. 2004). In the first observation, lasting about 9 ks, a narrow feature at $5.7^{+0.07}_{-0.12}$ keV was also detected with a confidence level of 96.3% (EW ∼ 70 eV, but with σ poorly constrained; the upper limit was found 0.28 keV). Even if the statistical significance is rather marginal, it is tempting to liken this feature with those reported in NGC 3516. However, we remind that the possibility cannot be ruled out that this feature is the red horn of a 'classical' double-peaked relativistic profile. Notice that 6.4 keV line with $\sigma = 140^{+120}_{-70}$ eV was also detected, which in this hypothesis would be interpreted as the blue horn of the broad relativistic line; see discussion in Guainazzi 2003.

In the second observation, a narrow ($\sigma < 0.1$ keV) feature is observed at 5.96 ± 0.05 keV (again besides a 6.4 keV line whose width is loosely constrained, $\sigma < 160$ eV; Bianchi et al. 2004), but only in the second half of the ∼ 20 ks observation (see Fig. 6). The feature is significant at 98.3% confidence level, and the EW is about 65 eV. The statistical

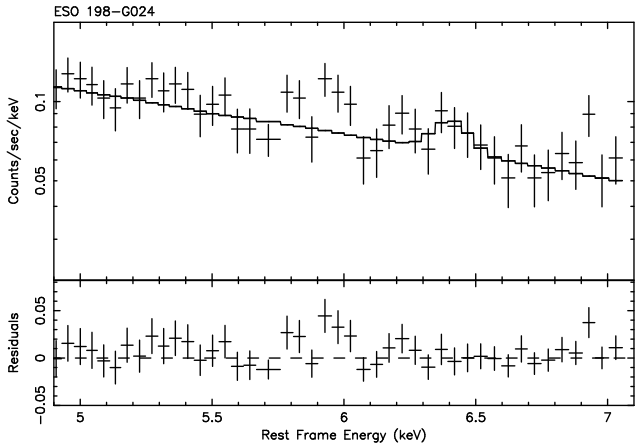

Figure 6. Best fit spectrum and residuals for the second half of the second *XMM–Newton* observation of ESO 198-G024. Energy is given with respect to the rest frame of the galaxy. The adopted model is a plain power-law plus a Gaussian line to reproduce the 6.4 keV line. Note the emission feature in residuals at ~ 5.96 keV.

significance of this feature is not very large, but its finding reinforces that of the previous observation.

One can assume that the 6.4 keV line is of different origin, possibly arising in the disc or in BLR. (This interpretation however seems to be incompatible with the line width in the first observation, which is at 90% confidence level inconsistent with the Hβ line width of 6400 km/s FWHM; Winkler 1992.) The other feature detected in both observations could be the blue horn of an annulus with $r \sim 6$, seen at low inclination (see Fig. 1 and Fig. 5). In that case the rest of the profile would be below detectability. Furthermore, assuming (as an order of magnitude estimate) that the visibility of the profile lasts for about a quarter of the orbit (which corresponds to roughly 10 ks), the resulting black hole mass is $M_\bullet \sim 10^8 M_\odot$. However, we stress again that, given the poor statistics, the above estimate should be taken more as a provisional hypothesis than as a reliable measurement.

A brief mention on the continuum variability is appropriate here. The line equivalent width for an isotropic illumination is about 150 eV (e.g. Matt et al. 1991). Given the observed value of EW, this means that the illuminating flare would account for about half the flux, and a ∼50% continuum variability would have been expected to accompany the feature variability, which instead is not observed. While stressing that the detection of the feature variability must be considered as tentative, a possible situation is that the illumination is very anisotropic and directed preferentially towards the disc (see e.g. Ghisellini et al. 1991).

3.3 NGC 7314

The Seyfert 1 galaxy NGC 7314 has a highly variable, broad iron line as observed by ASCA (Yaqoob et al. 1996). The source was then observed by the HETG onboard *Chandra*, and a narrow ($\sigma < 30$ eV) feature at 5.84 keV (EW = 20 eV) was discovered (Yaqoob et al. 2003) in the low state, after dividing the observation in two parts according to the count rate, even if with a moderate significance ($\sim 2\sigma$) only. As already noted by these authors, the narrow feature may be the blue horn from an annulus with $r \sim 6$ at small inclination angle (see Fig. 1 and Fig. 5). Another feature was also detected at 6.61 keV (EW = 30 eV); hence a viable alternative is that the latter feature represents the blue horn of emission from an annulus at $r \sim 50$ and low inclination angle, with the 5.84 keV being the red one, (see Fig. 5). The mass of the black hole is estimated to be $M_\bullet \sim 5 \times 10^6 M_\odot$ (Padovani & Rafanelli 1988), implying an orbital period of $T_{\rm orb} = 2.3$ ks at $r = 6$, and $T_{\rm orb} = 55$ ks at $r = 50$. The *Chandra* observation is ~ 100 ks long, and so both explanations are viable as far as orbital time scales are concerned. To discriminate between the two solutions, we re-analysed the *Chandra* observation, dividing it in three time intervals of equal duration about 30 ks. In each time interval the feature is barely visible, as expected (given the marginal detection) if the line flux is constant. This result therefore favours a small value of the orbital radius. However, given the limited quality of the data, no definitive conclusions can be drawn in this respect.

3.4 Mrk 766

Mrk 766 is one of the best studied narrow line Seyfert 1 galaxies. The presence of a broad, relativistic iron line in the spectrum of this source is, however, still an open issue. Page et al. (2001) found evidence for a relativistic line in the first *XMM–Newton* observation. On the other hand, subsequent reanalysis of the same data set, as well as of the second *XMM–Newton* observation (Pounds et al. 2003) did not provide evidence for such a line.

Turner et al. (2004) reported on the presence of a narrow feature at 5.6 keV during the first 100 ks of the second *XMM–Newton* observation, when the source was in a high state, and at 5.75 keV in the last 30 ks, after a sudden drop in flux. The EW of the 5.6 keV line is $\sim$ 15 eV, that of the 5.75 about 4 times higher. Turner et al. preferred explanation is in terms of a decelerating ejected blob. Let us instead discuss the system parameters in the orbiting spot hypothesis, even if the line and continuum variability are anticorrelated, contrary to what is expected in our model. Clearly, if the model is correct, continuum variability and illumination of the matter must be very complex.

Assuming again that the observed narrow feature corresponds to the blue horn, the emission must come from small radii to account for the significant redshift. The mass of the black hole in this source is estimated to be $10^7 M_\odot$ (Wandel 2002), corresponding to an orbital period of about 4.6 ks for $r = 6$, much less than observing times for both states. Hence we can assume that the line profile is averaged over several orbits. One possibility is that the inclination angle is very low, in which case we can neglect Doppler shifts. We find that the radius corresponding to the redshift-factor g of a spectral line is equal to $2/(1 - g^2)$ (in the Schwarzschild limit). The emission radius would then have been moved from about $r = 8.5$ in the first part of the observation to $r = 10.4$ in the second part. Increasing the inclination angle decreases the radius corresponding to a given g in the blue horn because of Doppler blueshift. For $\theta_{\rm o} = 30^\circ$ (see Fig. 5) the radius is already lower than 6, requiring a spinning black hole. Of course, at least part of the line shift may alternatively be due to ionization of the matter, which could also help explaining the larger equivalent width (e.g. Matt et al.

1996). Clearly, high throughput observations (capable of detecting line features in short exposure times) are necessary to break the degeneracy between r and $\theta_{\rm o}$.

4 CONCLUSIONS

We discussed the possibility that the narrow features in the 5–6 keV range, recently discovered in a few AGNs and usually interpreted as redshifted iron lines, could be due to illumination by localized orbiting spots just above the accretion disc. If this is indeed the case, these features may provide a powerful and direct way to measure the black hole mass in active galactic nuclei. To this aim, it is necessary to follow the line emission along the orbit. The orbital radius (in units of $r_{\rm g}$) and the disc inclination can be inferred from the variations of the line flux and centroid energy. Furthermore, $M_\bullet$ can be estimated by comparing the measured orbital period with the value expected for the derived radius. As shown in the previous section, present-day X-ray instruments do not have enough collecting area to perform this task accurately. This capability should be achieved by the planned high-performance X-ray missions such as *Constellation–X* and *Xeus*.

ACKNOWLEDGEMENTS

We thank A. Martocchia and the anonymous referee for useful comments. This paper is based partly on observations obtained with *XMM–Newton*, an ESA science mission with instruments and contributions directly funded by ESA Member States and the USA (NASA). VK and MD acknowledge support from grants GACR 205/03/0902 and 202/02/0735. SB and GM acknowledge financial support from Italian ASI and MIUR.

REFERENCES

Abramowicz A., Beloborodov A. M., Chen X.-M., Igumenshchev V., 1996, A&A, 313, 334
Artemova I. V., Björnsson G., Novikov I. D., 1996, ApJ, 461, 565
Bardeen J. M., Press W. H., Teukolsky S. A., 1972, ApJ, 178, 347
Bianchi S, Matt G., Balestra I., Guainazzi M., Perola G. C., 2004, A&A, to be submitted
Boller Th., Keil R., Trümper J., O'Brien P. T., Reeves J., Page M., 2001, A&A, 365, L134
Collin S., Coupé S., Dumont A.-M., Petrucci P.-O., Różańska A., 2003, A&A, 400, 437
Czerny B., Różańska A., Dovčiak M., Karas V., Dumont A.-M., 2004, A&A, submitted
Fabian A. C. et al., 2002, MNRAS, 335, L1
Fabian A. C., Iwasawa K., Reynolds C. S., Young A. J., 2000, PASP, 112, 1145
Ghisellini G., George I. M., Fabian A. C., Done C., 1991, MNRAS, 248, 14
Guainazzi M., 2003, A&A, 401, 903
Haardt F., Maraschi L., Ghisellini G., 1994, ApJ, 432, L95
Iwasawa K., Fabian A. C., Brandt N., Kunieda H., Misaki K., Terashima Y., Reynolds C. S., 1998, MNRAS, 295, L20
Karas V., 1996, ApJ, 470, 743
Lee J. C., Fabian A. C., Reynolds C. S., Brandt W. N., Iwasawa K., 2000, MNRAS, 318, 857
Madejski G. M., Done C., Turner T. J., Mushotzky R. F., Serlemitsos P., Fiore F., Sikora M., Begelman M. C., 1993, Nature, 365, 626
Markowitz A., Edelson R., Vaughan S., Uttley P., George I. M. et al., 2003, ApJ, 593, 96
Matt G., Fabian A. C., Ross R. R., 1996, MNRAS, 278, 1111
Matt G., Perola G. C., 1992, MNRAS, 259, 433
Matt G., Perola G. C., Piro L., 1991, A&A, 247, 25
Matt G., Perola G. C., Piro L., Stella L., 1992, A&A, 257, 63
Matt G., Perola G. C., Stella L., 1993, A&A, 267, 643
Merloni A., Fabian A. C., 2001, MNRAS, 328, 958
Miniutti G., Fabian A. C., Goyder R., Lasenby A. N., 2003, MNRAS, 344, L22
Misner C. W., Thorne K. S., Wheeler J. A., 1973, Gravitation (Freeman, San Francisco)
Nandra K., George I. M., Mushotzky R. F., Turner T. J., Yaqoob T., 1999, ApJ, 523, L17
Padovani P., Rafanelli P., 1988, A&A, 205, 53
Page M. J. et al., 2001, A&A, 365, L152
Porquet D., Kaastra J. S., Page K. L., O'Brien P. T., Ward M. J., Dubau J., 2003, A&A, 413, 913
Pounds K. A., Reeves J. N., Page K. L., Wynn G. A., O'Brien P. T., 2003, MNRAS, 342, 1147
Poutanen J., Fabian A. C., 1999, MNRAS, 306, L31
Reynolds C. S., Nowak M. A., 2003, PhR, 377, 389
Skibo J. G., 1997, ApJ, 478, 522
Semerák O., Karas V., A&A, 1999, 343, 325
Stella L., 1990, Nat, 344, 747
Thorne K. S., 1974, ApJ, 191, 507
Turner T. J. et al., 2002, ApJ, 574, L123
Turner T. J., Kraemer S.B., Reeves J.N., 2004, ApJ, in press
Wandel A., 2002, ApJ, 565, 762
Winkler H., 1992, MNRAS, 257, 677
Wu X.-B., Han J. L., 2001, ApJ, 561, L59
Yaqoob T., George I. M., Kallman T. R., Padmanabhan U., Weaver K. A., Turner T. J., 2003, ApJ, 596, 85
Yaqoob T., Serlemitsos P. J., Turner T. J., George I. M., Nandra K., 1996, ApJ, 470, L27